



# Dynamical scaling behavior of the Swift–Hohenberg equation following a quench to the modulated state

Q. Hou\*, S. Sasa, N. Goldenfeld

*Physics Department, 1110 West Green Street, University of Illinois, Urbana, IL 61801, USA*

---

## Abstract

We study the kinetics of phase transitions in a Rayleigh–Benard system after onset of convection using 2D Swift–Hohenberg equation. An initially uniform state evolves to one whose ground state is spatially periodic. We confirmed previous results which showed that dynamical scaling occurs at medium quench ( $\varepsilon=0.25$ ) with scaling exponents  $\frac{1}{5}$  and  $\frac{1}{4}$  under zero noise and finite noise, respectively. We find logarithmic scaling behavior for a deep quench ( $\varepsilon=0.75$ ) at zero noise. A simple method is devised to measure the proxy of domain wall length. We find that the energy and domain wall length exhibit scaling behavior with the same exponent. For  $\varepsilon=0.25$ , the scaling exponents are  $\frac{1}{4}$  and 0.3 at zero and finite noise, respectively.

*PACS:* 47.54.+r; 47.27.Te

*Keywords:* Scaling; Pattern formation

---

## 1. Introduction

The dynamics of pattern formation in systems away from equilibrium is a fascinating subject to study. There are numerous examples that exist in nature, such as Rayleigh–Benard convection, chemical reaction and biological pattern formation, etc. Much work [1] has been done on Rayleigh–Benard convection due to its relative simplicity. There, a fluid is confined between two horizontal plates which are heated from below. When the temperature difference is big enough such that the Rayleigh number  $R$  exceeds a critical value  $R_c$ , the fluid in the uniform state becomes unstable to one which consists of spatially periodic convection rolls. These rolls form domains with a typical size which grows with time. Swift and Hohenberg developed a simple model [2] to

---

\* Corresponding author.

describe this process. The order parameter equation reads,

$$\frac{\partial \psi}{\partial t} = \varepsilon \psi - \psi^3 - (1 + \Delta)^2 \psi + \eta,$$

where  $\psi$  is related to the vertically averaged magnitude of the velocity component normal to the plate. The reduced Rayleigh number  $\varepsilon = (R - R_c)/R_c$  measures how far the system is above the onset of convection. The thermal noise  $\eta$  satisfies the usual relation  $\langle \eta(x, t) \eta(x', t') \rangle = F \delta(x - x') \delta(t - t')$ . This model captures the three basic features of pattern formation in the Rayleigh–Benard system, namely, initial growth of the instability, its nonlinear saturation and development of a spatially periodic pattern.

Away from the threshold where  $\varepsilon \sim O(1)$ , one can perturb around the ground state  $\psi_0(x)$  which is periodic in  $x$  and define a phase  $\phi$  as in

$$\psi = \psi_0[\phi(\mathbf{x}, t)] + O(\zeta),$$

where  $\nabla \phi(\mathbf{x}, t) = \mathbf{q}(\mathbf{x}, t)$  and the gradients of local wavenumber  $\mathbf{q}$  are of the order of a small number  $\zeta$ . Thus one obtains the *phase equation* [3,4]. To lowest order in  $\varepsilon$ ,

$$\partial_t \phi = D_{\perp} \partial_{\perp}^2 \phi + D_{\parallel} \partial_{\parallel}^2 \phi,$$

where  $\perp$  and  $\parallel$  denotes directions along and normal to the rolls and the  $D$ 's are diffusion coefficients. Direct dimensional analysis tells us that the characteristic length grows as  $t^{1/2}$ . However,  $D_{\perp} \rightarrow 0$  due to local wavenumber relaxation. The next order expansion gives us a fourth order gradient term and one expects a scaling behavior  $L \sim t^{1/4}$  in the transverse direction (along the rolls) [1,5] which physically corresponds to curvature relaxation [6].

Scaling behavior is seen in numerical simulations. However, the exponent is  $\frac{1}{3}$  for noiseless case [6,7] and is apparently changed to  $\frac{1}{4}$  when finite noise is added [6]. Non-potential variants of the Swift–Hohenberg system which take into account of mean field flow give the same result [7] (non-uniform horizontal motion of the fluid, important for fluid with small viscosity).

The fact that the phase equation predicts a different value of exponent from simulation and that the exponent is noise dependent is intriguing. Actually, since the phase equation starts from perturbation around an ideal state, it fails to encompass the many defects that are present in a real system. However, the coarsening process in pattern formation is brought about by defect movement. Through defect annihilation, larger domains of nearly ideal configuration form at the expense of smaller ones. This important role played by defects is well-known; a good example is the kinetics of the formation of the Meissner state in a type II superconductor at zero field [8], where the inter-vortex potential  $U(r)$  determines the scaling behavior of the inter-vortex distance.

## 2. Numerical results

We approach the problem primarily as numerical experimentalists. We try to measure strategic quantities which could shed light on the mechanism of the pattern coarsening,

especially quantities which could be related to defects in the system. We use an explicit, first order accurate, pseudospectral method. The boundary is periodic to simulate large aspect ratio systems. Two  $\varepsilon$  values are used. For  $\varepsilon=0.25$ , the lattice is 512 by 512, time step size is 0.1. For  $\varepsilon=0.75$ , the lattice is 256 by 256, time step size is 0.05. In either case, there are 8 lattice points per ideal period. In the case of  $\varepsilon=0.25$ , we also did a case with finite noise to study the effect of noise on the dynamics. To obtain the statistics, each run is repeated with 10 different initial random configurations to average over.

#### A. $\varepsilon=0.25$

We measure three quantities. One is the structure factor  $S(k)$ . This is the canonical measure from which one can calculate the dynamical scaling exponents. We also measure the energy of the system as well as the sum of all the domain wall lengths. The former could signal, in this relaxational model, whether bulk or defects are contributing most to energy relaxation, while the latter could give us information on defect dynamics.

The structure factor is defined as the statistical average of the fourier spectrum of the equal time correlation function, averaged over all directions of the 2D wave vector,

$$S(k) = FT \langle \psi(x, t) \psi(x', t') \rangle.$$

The Swift–Hohenberg system belongs to the  $I_s$  instability class [1]. Accordingly,  $S(k)$  is peaked at  $k=k_0$  away from the origin, corresponding to the ground state and most unstable mode above onset of convection. Due to the nonlinear interaction, there are peaks corresponding to higher harmonics present in  $S(k)$ . Away from these higher harmonics, it is observed that  $S(k)$  is a function of  $|k^2 - k_0^2|$ . We fit  $S(k)$  to squared Lorentzian form [7]

$$S(k) = \frac{S(k_0)}{(1 + (\Gamma(k^2 - k_0^2))^2)},$$

where  $S(k_0)$  is the peak amplitude and  $\Gamma$  is a fitting parameter from which one can calculate  $L$ , the characteristic width of  $S(k)$ . The two parameters  $S(k_0)$  and  $L$  exhibit scaling behavior. The exponents are consistent with results obtained by earlier workers.

$$L \sim S(k_0) \sim t^{\phi_L}, \quad \phi_L = \begin{cases} \frac{1}{5}, & F_d = 0, \\ \frac{1}{4}, & F_d = 0.05, \end{cases} \quad (1)$$

where we define the discretized noise  $F_d = F/(\Delta x)^2$ , where  $\Delta x = \pi/4$  is mesh size used in our simulation. The data plots for  $S(k_0)$  and  $L$  are shown in Fig. 1.

Using these characteristics, we scale the structure factor from different times. The central region of  $S(k)$  collapses onto a universal curve (Fig. 2). It is interesting to notice that  $S(k_0)$  scales as  $L$  [6] not  $L^2$  as is the usual case for phase ordering in a 2D system. This is due to the fact that, in the process of Fourier transformation

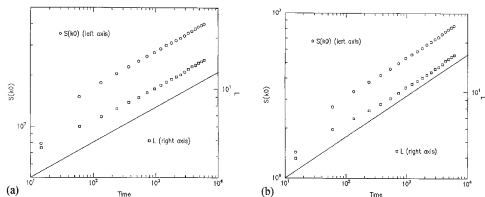


Fig. 1.  $L/S(k_0)$  vs. Time ( $F_d = 0$ , left and  $F_d = 0.05$ , right). Left and right reference lines have slopes and  $\frac{1}{4}$ , respectively.

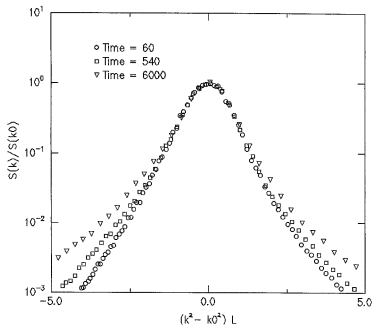


Fig. 2. Scaled  $S(k)$  vs.  $k^2 - k_0^2$ . Noiseless.

$S(\vec{r}) \rightarrow S(\vec{k})$ , most of the contribution comes from annulus  $k_0 dk$  instead of area  $k dk$  at the origin where  $k \sim dk$ . Since  $\Gamma$  is basically  $L$ , we write the scaling form of  $S(k)$  as

$$S(k) = L l f(L l |k^2 - k_0^2|),$$

where  $l$  is a constant length to give the right dimension, proportional to the periodicity.

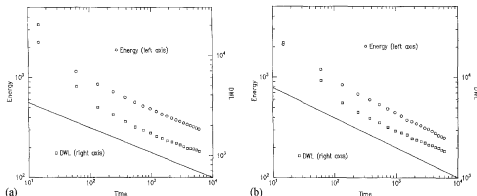


Fig. 3.  $E/DWL$  vs. Time ( $F_d = 0$ , left and  $F_d = 0.05$ , right). Left and right reference lines have slopes  $\frac{1}{4}$  and 0.3, respectively.

There is an energy functional  $H$  in our model, where

$$H = \frac{1}{2} [(1 + \Delta)\psi]^2 - \frac{1}{2} \varepsilon \psi^2 + \frac{1}{4} \psi^4.$$

The system evolves in a way such that the energy is decreasing as a function of time. The questions then are: Is there energy scaling? If so, what is the scaling exponent? And is it related to the scaling of the characteristic length  $L$ ? Scaling in energy was observed in other systems such as phase ordering in nematic films [9] where it is found to be mostly due to bulk energy relaxation.

The ground state energy density can be easily calculated to be  $-\frac{1}{2}\varepsilon^2$  to the lowest order in  $\varepsilon$ . In the noiseless case, this is also the long time limit. We can measure the excess energy  $E$  of the system relative to that of its ground state. For the noisy case, it is a bit tricky, because there is a ‘thermal’ energy component from the external noise source. So the long time limit is unknown. What we did was to determine this value empirically by fitting the energy evolution to a power law allowing for an offset. Then excess energy is found by subtracting this offset. Whether this is a good fit is answered by seeing whether the scaling prevails over several decades.

Indeed, a nice scaling regime is found. However, the scaling exponent is not related to that of the characteristic length  $L$  in any simple way (such as  $L^{-2}$  as expected from ordinary bulk relaxation). We think the dominant contribution comes from defects as will be discussed below. Our results are shown in Fig. 3, and may be summarized as

$$E \sim t^{-\phi_E}, \quad \phi_E = \begin{cases} \frac{1}{4}, & F_d = 0, \\ 0.3, & F_d = 0.05. \end{cases} \quad (2)$$

An accurate measurement of domain wall lengths should be very helpful in clarifying one of our main concerns: what is the role of defects? However, it is quite difficult to determine where a domain wall is located mathematically. Other researchers have used optical filtering procedures to visualize domain walls [10]. However, no attempt

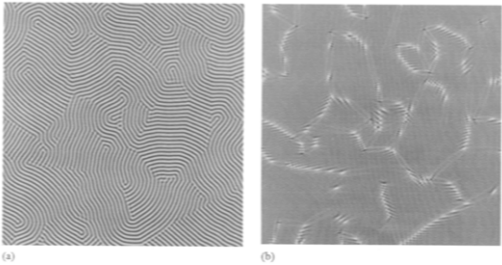


Fig. 4. Order parameter configuration (left) and converted amplitude  $A$  squared (right).

has been made to measure the length of these domain walls. Furthermore, the filtering procedure is very computationally intensive.

We devised a simple method to identify domain walls and obtained a proxy of the domain wall lengths. The method is based on the observation that, within a domain, the order parameter configuration is close to the ground state solution,  $\psi \sim A \sin \mathbf{k}_0 \cdot \mathbf{x}$ . We have  $\nabla \psi \sim A \mathbf{k}_0 \cos \mathbf{k}_0 \cdot \mathbf{x}$  and  $A^2 \sim \psi^2 + (\nabla \psi)^2 / k_0^2$ . The converted amplitude  $A$  is almost constant everywhere except at grain boundaries (Fig. 4). Thus grain boundaries can be located by filtering with respect to  $A$ .

We set up a threshold so that, if the calculated  $A^2$  is bigger than  $0.7 \times \text{Max}(A^2) + 0.3 \times \text{AVG}(A^2)$  or smaller than  $0.7 \times \text{Min}(A^2) + 0.3 \times \text{AVG}(A^2)$ , that point is counted as belonging to a domain wall. The length proxy  $DWL$  is defined as a count of all such points. Again, scaling behavior is observed for  $DWL$ . The exponent is different from that of the characteristic length  $L$ . Instead, it is the same as that of the energy relaxation (Fig. 3) ( $DWL$  for noiseless case was an average of 5 runs since we devised the above way of measuring  $DWL$  after the first 5 runs). This strongly suggests that excess energy is primarily distributed at domain walls and other defects. This part of the energy relaxes slowly, via defect annihilation. On the other hand, bulk energy is the fast mode and scales as  $L^{-2} \sim t^{-2/5}$  and decays much faster than the excess energy  $E$ . At this point, it is tempting to conclude that defects are indeed the driving force behind the coarsening process due to its dominant contribution to the excess energy. However, it is still not clear how one could link the evolution of  $E$  and  $DWL$  with the growth of  $L$ .

$$DWL \sim t^{-\phi_{DWL}}, \quad \phi_{DWL} = \begin{cases} \frac{1}{4}, & F_d = 0, \\ 0.3, & F_d = 0.05. \end{cases} \quad (3)$$

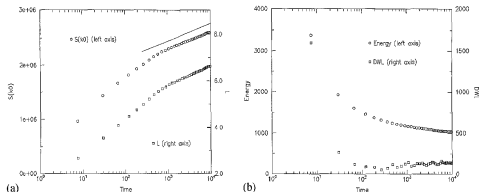


Fig. 5.  $L/S(k_0)$  vs Time (left) and  $E/DWL$  vs Time (right).

### B. $\varepsilon = 0.75$

For large  $\varepsilon$ , the system is much further away from equilibrium. We anticipated that there would be more isolated dislocations and they could give rise to a different coarsening process. This is indeed what we found. The system evolves slowly. The characteristic length exhibits logarithmic scaling behavior, while the excess energy decays even slower and the number of defects stays almost constant (Fig. 5).

$$L \sim S(k_0) \sim \log t, \quad F_d = 0.$$

A heuristic argument for the logarithmic behavior uses the fact that the pair potential [11] between two dislocations is exponentially decaying with respect to the distance between them, namely,

$$U = \frac{U_0}{\sqrt{z/\lambda}} \exp\left(-\frac{x^2}{z\lambda}\right). \quad (4)$$

Setting  $r \sim x \sim z$ , one has, for the damped defect motion,

$$\eta \frac{dr}{dt} = -\frac{dH}{dr} = -\frac{v_0}{\sqrt{r/\lambda}} \exp\left(-\frac{r}{\lambda}\right). \quad (5)$$

The leading order of the solution to above equation gives us logarithmic behavior. Now substitute this leading order behavior  $r \sim \log(t)$  into the defect pair potential energy, one finds that the pair potential energy part scales as  $t^{-1}$ , much faster than what one sees in the  $E$  vs Time plot shown above. Thus, there must be other significant energy sources which could be some energy background not important to dynamics.

### 3. Conclusions

In this paper, we presented results from our numerical simulation of the Swift–Hohenberg system. For a medium quench ( $\varepsilon = 0.25$ ), the system has many domain

wall defects. We confirmed the dynamic scaling behavior in structure factor observed by previous researchers. We showed that the energy of the system also exhibits scaling behavior. Its scaling exponent does not have a simple relationship with that of the characteristic width, making it difficult to draw any concrete conclusion. However, one notices that the energy relaxation is slower than what one would expect from bulk contribution, namely,  $L^{-2}$ . We devised a simple way to measure the proxy of domain wall length. The *DWL* has the same scaling exponents as the energy, suggesting that energy is concentrated on defects. This is consistent with the notion that defects are the driving force behind the coarsening process. We find that adding noise into the system speeds up the evolution, because all the exponent values increase.

For a deep quench ( $\varepsilon=0.75$ ), we see a much slower coarsening process where there are mostly isolated dislocations in the system. The characteristic length scale shows logarithmic behavior. To explain this, we give a heuristic argument assuming overdamped isotropic dynamics under the influence of the pair potential between defects.

### Acknowledgements

This work is supported by grant NSF-DMR-93-14938 and NSF-DMR-89-20538.

### References

- [1] M. Cross and P. Hohenberg, *Rev. Mod. Phys.* 65 (1994) 851.
- [2] J. Swift and P. Hohenberg, *Phys. Rev. A* 15 (1977) 319.
- [3] Y. Pomeau and P. Manneville, *J. Phys. Lett.* 40 (1979) L-609.
- [4] T. Passot and A. Newell, *Physica D* 74 (1994) 301.
- [5] M. Cross and A. Newell, *Physica D* 10 (1984) 299.
- [6] K. Elder, J. Vinals and M. Grant, *Phys. Rev. Lett.* 68 (1992) 3024.
- [7] M. Cross and D. Meiron, preprint, 1995.
- [8] F. Liu, M. Mondello and N. Goldenfeld, *Phys. Rev. Lett.* 66 (1991) 3071.
- [9] M. Zapotocky, P. Goldbart and N. Goldenfeld, *Phys. Rev. E* 51 (1995) 1216.
- [10] M. Cross, D. Meiron and Y. Tu, *Chaos* 4 (1994) 607.
- [11] J. Toner and D. Nelson, *Phys. Rev. B* 23 (1981) 316.